Biochar mineralization and priming effect on SOM decomposition in two European short rotation coppices

MAURIZIO VENTURA[1], GIORGIO ALBERTI[2,3], MAUD VIGER[4], JOSEPH R. JENKINS[4], CYRIL GIRARDIN[5], SILVIA BARONTI[6], ALESSANDRO ZALDEI[6], GAIL TAYLOR[4], CORNELIA RUMPEL[5], FRANCO MIGLIETTA[2,6,7] and GIUSTINO TONON[1,2]

[1]Faculty of Science and Technology, Free University of Bolzano/Bozen, Piazza Università 1, 39100 Bolzano, Italy, [2]MountFor Project Centre, European Forest Institute, Via E. Mach 1, San Michele a/Adige, Trento 38010, Italy, [3]Department of Agricultural and Environmental Sciences, University of Udine, Via delle Scienze 206, 33100 Udine, Italy, [4]Centre for Biological Sciences, University of Southampton, Life Science Building, Highfield Campus, Southampton SO17 1BJ, UK, [5]BIOEMCO, UMR 7618, CNRS-INRA-ENS-Paris 6, Bâtiment EGER, Aile B, 78820 Thiverval-Grignon, France, [6]IBIMET-CNR Institute of Biometeorology, National Research Council, Via Caproni 8, 50145 Firenze, Italy, [7]FoxLab, Forest & Wood Science, Fondazione E. Mach, Via E. Mach 1, San Michele a/Adige, 38010 Trento, Italy

Abstract

As studies on biochar stability in field conditions are very scarce, the carbon sequestration potential of biochar application to agricultural soils remains uncertain. This study assessed the stability of biochar in field conditions, the effect of plant roots on biochar stability and the effect of biochar on original soil organic matter (SOM) decomposition in two (Italy and United Kingdom) short rotation coppice systems (SRCs), using continuous soil respiration monitoring and periodic isotopic ($\delta^{13}CO_2$) measurements. When root growth was excluded, only 7% and 3% of the biochar carbon added was decomposed after 245 and 164 days in Italy and United Kingdom sites respectively. In the presence of roots, this percentage was increased to 9% and 8%, suggesting a small positive priming effect of roots on biochar decomposition. A decreased decomposition rate of original SOM was observed at both sites after biochar incorporation, suggesting a protective effect of biochar on SOM. This study supports the carbon sequestration potential of biochar and highlights the role of root activity on biochar decomposition, questioning the applicability of laboratory incubation studies to assess biochar stability.

Keywords: biochar, char, carbon sequestration, gasification, poplar, priming effect, roots, soil organic matter

Received 28 March 2014; revised version received 20 June 2014 and accepted 23 July 2014

Introduction

Biochar is a carbon-rich material produced from pyrolysis or gasification of biomass under low oxygen conditions (Lehmann, 2007). Biochar application to agricultural soils has been proposed as a promising strategy for carbon (C) sequestration (Lehmann, 2007) and climate change mitigation. However, the potential of biochar to improve soil C-sink is still under debate, since its stability seems to depend on several factors, such as the starting feedstock, pyrolysis conditions, soil environment and vegetation cover of the site (Hilscher & Knicker, 2011). Several short-term incubation experiments (Hamer *et al.*, 2004; Cheng *et al.*, 2008a; Kuzyakov *et al.*, 2009; Zimmerman, 2010) suggest centennial or millennial mean residence times for biochar stability. Other authors found a faster decomposition rate (Bird *et al.*, 1999; Nguyen & Lehmann, 2009; Zimmermann

et al., 2012) and a rapid transformation of biochar by abiotic and biotic oxidation (Hamer *et al.*, 2004; Bruun *et al.*, 2008; Hilscher *et al.*, 2009; Hilscher & Knicker, 2011; Zimmermann *et al.*, 2012). Contrasting results also exist on the effect of biochar on the stability of native soil organic matter (SOM) (Kuzyakov *et al.*, 2000). Some studies reported a stimulation (Wardle *et al.*, 2008; Cross & Sohi, 2011; Zimmerman *et al.*, 2011) and others no effect or inhibition (Kuzyakov *et al.*, 2009; Novak *et al.*, 2010; Spokas, 2010; Singh & Cowie, 2014) of native SOM decomposition after biochar addition to soil. Climate, especially temperature, can strongly affect both biochar and SOM decomposition rate (Cheng *et al.*, 2008a; Nguyen *et al.*, 2010). Zimmerman *et al.* (2011) reported that the direction (positive or negative) of the priming effect and its magnitude depend on soil and biochar type, ranging from −52 to 89% 1 year after soil biochar application.

Most of the experiments on biochar stability are based on short-term lab incubations while field studies remain scarce (Jones *et al.*, 2012; Gurwick *et al.*, 2013). There-

Correspondence: Maurizio Ventura, tel. +39 0471 017806, fax +39 0471 017009, e-mail: maurizio.ventura@unibz.it

fore, little is known about the interactions between biochar and roots and the related effects on biochar stability (Ventura *et al.*, 2013).

The overall aim of this study was to assess, the C sequestration potential of biochar under field conditions. In particular, we aimed to assess: (i) the stability of biochar in field conditions; (ii) the effect of biochar application on SOM decomposition (iii) the effect of plant roots on biochar stability. To achieve these aims, two different field experiments were carried out in Italy and the United Kingdom in two short rotation coppice systems (SRCs). This choice was made because of the increasing importance of SRC as one of the most efficient agricultural systems to meet European greenhouse gas reduction targets (Don *et al.*, 2012). Moreover, the use of biochar in agriculture for food production is still debated, because of the high content of polycyclic aromatic hydrocarbons (PAHs), that could have negative impacts on the soil biota and human health (Brown *et al.*, 2006), if translocated to the edible part of the plant and also because of possible negative effects of biochar on plant defence chemistry (Viger *et al.*, 2014). Biochar application to non-food bioenergy crop systems avoids this issue of toxicity and at the same time focuses on a land use change that may be of wide significance in the future.

Materials and methods

Experimental sites

In Italy, the experimental field was set up in a poplar (*Populus x Canadensis* Mönch, Oudemberg genotype) SRC plantation with a 2-year rotation period, located in Prato Sesia (Novara) (45° 39′ 32.2812″ N; 8° 21′ 16.8339″ E). The plantation was established in the spring of 2010 with a density of 6600 trees ha^{-1} in single rows with a 3 m distance between rows and 0.5 m between plants on the row. Coppicing was undertaken in the spring of 2012 before biochar application. The soil is sandy loam (12% clay, 34% silt, 54% sand) with a pH of 5.4. Climate is temperate with an average annual temperature of 12 °C and an average annual precipitation of 1500 mm.

The UK experimental site consists of a SRC plantation of mixed willow genotypes (*Salix spp.*), located at Pulborough, West Sussex, UK (50°57′ N; 0°30′ W). The plantation was established in 2008 with a density of 15 000 trees ha^{-1} in double rows with alternating distances of 0.75 and 1.4 m between the rows and 0.55 m in the row. The soil is silt loam (7% clay, 53% silt, 40% sand) with a pH of 5.5. Climate is temperate with an average annual temperature of 11 °C and an average annual precipitation of 800 mm. Coppicing was performed in the spring of 2009.

Biochar application

The biochar used in the two experiments was produced from maize (*Zea mays* L.) silage feedstock pellets at 1200 °C under atmospheric pressure with a residence time of 40 min in a gasification plant (©A.G.T. – Advanced Gasification Technology s.r.l., Cremona, Italy). Table 1 reports the main physicochemical characteristics of the biochar used in the experiments. Biochar C, N and H contents were determined by CHN elemental analyzer (Flash EA 2000 Thermo Fisher Scientific, Bremen, Germany). Nutrient content was determined with an inductively coupled plasma optical emission spectrometer (ICP–OES), after mineralization with an Ethos TC microwave labstation (Milestone, Bergamo, Italy). Biochar δ^{13}C was determined with a continuous flow isotopic ratio mass spectrometer (CF-IRMS; Delta V Advantage, Thermo Fisher Scientific, Bremen, Germany).

A completely randomized design with two treatments (biochar (B) and control (C)) and four replicates (plots) per treatment was used at both sites. Plots (45 m^2 each) were designed to include three plant rows and nine plants per row. Biochar (30 t ha^{-1}) was incorporated into the first 15-cm soil layer by rotary hoeing on March 30th 2012 at the Italian site and on June 19th 2012 by hand at the UK site. To disturb the soil evenly in control and biochar-treated plots, hoeing or digging was carried out in both control and treatment plots.

Soil respiration measurements

Total and heterotrophic soil respiration was measured in biochar-treated ($R_{tot}B$ and R_hB, respectively) and control plots (R_{tot} and R_h, respectively). The trenching method was used to measure R_h and R_hB (Hanson *et al.*, 2000). On February 2012, at

Table 1 Biochar physicochemical characteristics

Parameter	Unit	
Bulk density	g cm^{-3}	1.41
pH (H$_2$O)	–	11.6
ash (550 °C)	% DM	39.3
salinity	mS m^{-1}	758
H	%	2.3
H/C atomic ratio	–	0.5
C	%	56.1
N	%	1.35
C:N	–	42.9
δ^{13}C	‰	-13.8
Ca	g kg^{-1}	38.1
K	g kg^{-1}	32.3
Mg	g kg^{-1}	9.4
Al	g kg^{-1}	4.27
Fe	g kg^{-1}	3.12
Mn	mg kg^{-1}	211.3
Zn	mg kg^{-1}	183.1
Sr	mg kg^{-1}	148.1
Cu	mg kg^{-1}	46.30
Si	mg kg^{-1}	25.45
P	mg kg^{-1}	8.56
Na	mg kg^{-1}	1.70
S	mg kg^{-1}	1.32

the Italian site, six trenched subplots (50 × 50 cm) were set up, three per each treatment, by digging 60-cm deep and 15-cm-wide trenches. Before refilling the trenches with the original soil, each subplot was isolated with a geotextile canvas (Typar®, Dupont, Wilmington, DE, USA) to prevent root growth into the trenched plot, and allow gas and water exchanges. At the UK site, the trenched plots were isolated with a root exclusion stainless-steel cylinder open at both ends (32 cm diameter, 40 cm height), which was pushed into the ground undisturbed.

At each site, soil CO_2 efflux was measured in three of the four plots per treatment using a closed dynamic soil respiration system with 12 automated chambers (Delle Vedove *et al.*, 2010) every 2 and 4 h at the Italian and UK site, respectively. The difference in sampling frequency was related to the different power supply available at each site (i.e. AC for Italy and batteries with solar panels for United Kingdom). The system uses the rate of increase in CO_2 within the chamber to estimate the rate at which CO_2 diffuses into free air outside the chamber. To minimize the underestimation of the efflux due to the alteration of the diffusion gradient, we used nonlinear curve fitting. Specifically, after chamber lid closure, when a steady gas mixing within the chamber was established (typically after 30–40 s) a nonlinear regression between CO_2 concentration and time was performed (Delle Vedove *et al.*, 2010). CO_2 concentration data were plotted against time for each chamber and measurement. CO_2 concentration trends were checked for their curvature and final CO_2 value. If curvature was not convex and/or the difference between initial and final CO_2 concentrations was below 3 ppm, final computed fluxes were discarded. When it was impossible to estimate nonlinear regression parameters because of the linearity of CO_2 increase with time, a linear model was then used. If the coefficient of regression (R^2) was below 0.90, computed fluxes were discarded.

One chamber was installed in each plot to measure R_{tot} and another chamber was installed on each root exclusion subplot, to measure R_h. The chambers were installed in the central part of each plot, in the middle between two tree rows, and placed on stainless-steel collars (20 cm diameter, 8 cm height) inserted for 4 cm into soil. The exact volume was calculated for each chamber after insertion into soil, by measuring chamber height from soil surface.

Soil temperature (T) at 10 cm depth and soil water content (SWC) between 0 and 18 cm were recorded every 30 min using temperature probes, (107, Campbell Scientific, Logan UT, USA) and water content reflectometers (CS-616, Campbell Scientific, Logan UT, USA), respectively. The probes were installed close to soil respiration chambers. In the Italian site, soil temperature and SWC were measured in each plot and trenched subplot. In the UK site, soil temperature was measured in trenched and untrenched soil, while SWC was measured only in the untrenched soil. A meteorological station was available at each field site for measurements of air temperature and humidity (CS215 Probe, Campbell Scientific, Logan, UT, USA) and rainfall (52202 Tipping Bucket Rain gauge, R. M. Young Company, Traverse City, Michigan, USA). Soil respiration measures were averaged on a daily basis per plot, subplot (trenched and untrenched) and treatment (B and C).

Only daily averages based on at least six of the 12 measurements (Italy) and three of the six measurements (United Kingdom) valid soil respiration measurements per day and on at least three replicates per treatment (B and C) and subplot (trenched and untrenched) were considered. Distribution of daily flux coefficient of variation (CV) was computed by treatment and subplot. Soil respiration daily fluxes with CV higher than 90th percentile were discarded.

Missing or discarded data were gap-filled according to the following model proposed by Qi & Xu (2001):

$$R = aT^b \cdot SWC^c \tag{1}$$

where R is the soil CO_2 efflux (total or heterotrophic), T is the soil temperature (°C) and SWC is the soil water content (%). In the UK site, SWC data were not available in the period from June 19, 2012 to August 14, 2012. For this short-time period, gap-filling of soil respiration data was done according to a single exponential model ($R=aT^b$)

The models were parameterized using soil temperature and soil moisture data collected in the experimental sites, determining parameters a, b and c for each site and soil respiration chamber by a nonlinear regression analysis. Finally, cumulative soil respiration fluxes were calculated for each chamber over the whole experimental period. All the CO_2 fluxes were expressed as g C m^{-2}.

Isotopic measurements and Keeling plots

The isotopic signature ($\delta^{13}C$) of the respired CO_2 was periodically assessed using the Keeling plot method (Ngao *et al.*, 2005; Joos *et al.*, 2008). Manual sampling of respired CO_2 followed by isotopic ratio mass spectrometer analysis (IRMS) and direct on-line sampling using a Picarro G2131-i $\delta^{13}C$ High-precision Isotopic CO_2 Cavity Ring Down Spectrometer (CRDS) were used and compared at both sites.

Manual sampling was performed using a portable infrared gas analyzer (IRGA, EGM 4, PP-Systems, Amesbury, MA, USA) connected to a closed dynamic chamber (SRC 1, PP Systems) and to a set of eight three-way valves (Fig. 1). The valves allowed air to circulate through four glass vials (12 ml exetainer gas vials Labco Ltd., Lampeter, Ceredigion, UK) or alternatively bypass them. At the beginning of the sampling cycle, all four vials where connected to the circuit and the valves were opened to allow the air to circulate through all of them. The chamber was placed on the soil surface and the four vials were filled sequentially during the accumulation of the respired CO_2 into the system. Before collecting each vial, they were isolated from the circuit by closing the corresponding valves. CO_2 concentration and time since the beginning of the measurement cycle were also recorded. A minimum range of 300 ppm between the first and the last air sampling was kept to properly calculate $\delta^{13}C$ of soil-respired CO_2 using the Keeling plot method (Joos *et al.*, 2008). For each sampling cycle, the chamber was kept on the soil for a time ranging from 10 to 20 min, depending on soil CO_2 emission rate. Three sampling cycles were performed in three different positions around each automated soil respiration chamber (for a total of 36 keeling plots
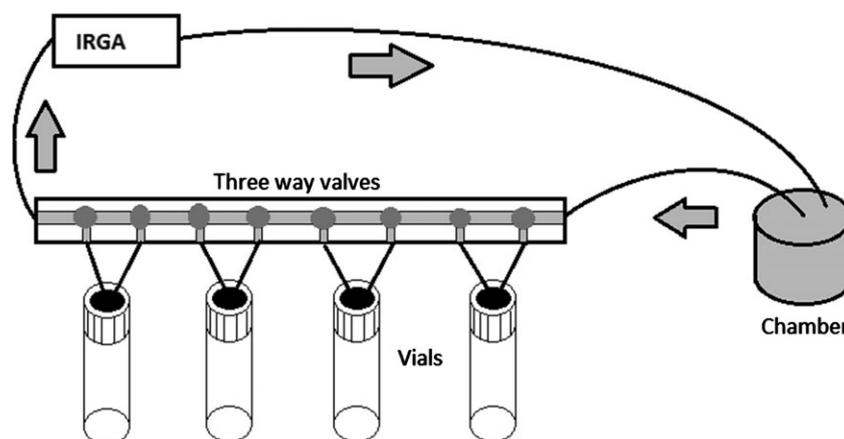
Fig. 1 Scheme of the sampling system used to collect CO_2 emitted from the soil to calculate $\delta^{13}C$ of soil-respired CO_2 by Keeling plot method. Arrows indicate the movement of the air through the system.

per sampling day, nine per treatment). The collected vials were then analysed in the lab for $\delta^{13}CO_2$ value with a continuous flow isotopic ratio mass spectrometer (CF-IRMS; Delta V Advantage, Thermo Fisher Scientific, Bremen, Germany) coupled with a gas purification device (Gas-Bench II; Thermo Fisher Scientific, Bremen, Germany).

The CRDS measurements were performed by connecting the analyzer to the automated soil respiration system to subsample the circulating air. Instantaneous CO_2 concentration and $\delta^{13}CO_2$ were recorded every 1 s by the CRDS in the CO_2 concentration range between 500 and 1200 ppm. Measurement cycles, lasting 10–20 min each, were repeated in three different positions in the soil around each automated soil respiration chamber on each sampling day.

At the Italian site, monthly eight manual and two CRDS sampling campaigns were performed between April and November 2012. At the UK site, two CRDS measurements (on August 14, 2012 and October 2, 2012) and one manual sampling (on March 7, 2012) were performed. Preliminary tests (Figure S1) in a $\delta^{13}CO_2$ range between $-28‰$ and $-19‰$ showed a good correlation ($R = 0.85$, $P < 0.05$) between the two methods (IRMS manual sampling vs. on-line CRDS measurements). According to major axis regression analysis, the intercept and slope of the regression line were not significantly different from 0 and 1, respectively. Regardless, the difference we detected between IRMS manual sampling and on-line CRDS measurements could be related to pressure anomalies within the chamber during CRDS sampling. This effect could have led to biases in the $\delta^{13}CO_2$ of soil respiration by affecting the ratio of $^{13}CO_2$ to $^{12}CO_2$ that diffused across the soil-atmosphere interface. However, we were not able to quantify such an error as there is no theoretical analysis available for such an effect presently (Takahashi & Liang, 2007). Therefore, the following equation was used to convert CRDS in IRMS data:

$$\delta^{13}CO_2\text{IRMS} = -3.05 + 0.81\delta^{13}CO_2\text{CRDS} \qquad (2)$$

where $\delta^{13}CO_2\text{ CRDS}$ and $\delta^{13}CO_2\text{ IRMS}$ and are the isotopic signatures of CRDS- and IRMS-derived data, respectively.

Biochar decomposition and priming effect on SOM

The fraction of CO_2 respiration derived from the biochar decomposition (f_B) was calculated for both $R_{tot}B$ and R_hB using a mass balance approach according to Phillips & Gregg (2001):

$$f_B = \frac{\delta^{13}CO_{2B} - \delta^{13}CO_2\text{SOM}}{\delta^{13}C_B - \delta^{13}CO_2\text{SOM}} \qquad (3)$$

where $\delta^{13}CO_{2B}$ and $\delta^{13}CO_2\text{SOM}$ are the isotopic signatures of the CO_2 emitted from B and C, respectively, and $\delta^{13}C_B$ is the isotopic signature of biochar ($\delta^{13}C = -13.8‰$).

Assuming a linear variation in f_B between two Keeling plot sampling dates, the daily biochar-derived CO_2 fluxes were obtained multiplying f_B by the daily soil CO_2 fluxes of R_hB and $R_{tot}B$. Cumulative biochar-derived CO_2 flux was then calculated over the whole experimental period for both trenched ($R_{h\text{-biochar-derived}}$) and untrenched subplots ($R_{tot\text{-biochar-derived}}$) by summing the single daily biochar-derived CO_2 fluxes. $R_{h\text{-biochar-derived}}$ and $R_{tot\text{-biochar-derived}}$ were then used to estimate the amount of C remaining in comparison with that was originally present in the biochar matrix. The priming effect of root activity ($P_{eff\text{-root}}$) on biochar decomposition was calculated as follows:

$$P_{eff-root} = R_{tot-biochar-derived} - R_{h-biochar-derived} \qquad (4)$$

In biochar-treated plots, the cumulative flux derived from the decomposition of native soil organic matter ($R_{h\text{-SOM-derived}}$) was calculated as follows:

$$R_{h-SOM-derived} = R_hB - R_{h-biochar-derived} \qquad (5)$$

The priming effect of biochar ($P_{eff\text{-biochar}}$) on SOM decomposition was calculated only in the trenched plots as follows:

$$P_{eff-biochar} = R_{h-SOM-derived} - R_h \qquad (6)$$

Statistical analysis

All statistical analysis, soil respiration elaborations and flux computations were performed in STATA 10.1 (© StataCorp, College Station, TX, USA). Cumulative soil respiration fluxes

measured on biochar-treated and control plots were compared using analysis of variance (ANOVA), considering biochar application, trenching treatments and their interaction. Similarly, $\delta^{13}C$ of the respired CO_2, for each single date, were compared by ANOVA. Homogeneity of variance was checked before analysis. Intercepts of the Keeling plots were calculated using least squares linear regression. Major axis regression was used to compare results from Keeling plots obtained with manual sampling and CRDS measurements. Soil temperature and water content data were compared by repeated measures ANOVA using SigmaPlot 12 (Systat Software, Inc., USA).

Results

The model used to gapfill the missing soil respiration data on the base of soil temperature and water content showed a high predictive capacity ($R^2 = 0.72$ for the Italian site and 0.90 for the UK site, on average), which allowed us to recover most of the missing data. The model including only soil temperature showed a lower R^2 (0.42 on average). However, this model was used to gap-fill data only for a short-time period. Including both measured and gap-filled data, the dataset accounted for the 94% and 92% of the expected daily data for the Italian and UK sites, respectively. Residual gaps were due to power failure, which did not allow us to record soil water content and soil temperature data.

Biochar treatment significantly increased SWC in the two experimental sites (Figs 2c, d and 3b). In the Italian site, trenching affected SWC and soil temperature depending on the presence of biochar. In the summer period, when biochar was applied, SWC was significantly higher in the trenched than in control plots (Fig. 2d). In the same period, also soil temperature was affected by trenching in presence of biochar, being slightly but significantly lower in trenched than control plots (Fig. 2b). On the contrary, when biochar was not applied, SWC in the trenched plots was slightly but significantly lower than in untrenched soil (Fig. 2c). Daily total and heterotrophic respiration measured in control (R_{tot}, R_h) and biochar-treated plots ($R_{tot}B$ and R_hB) at both sites (Fig. 4) showed a typical annual variation with higher values in summer due to the higher soil temperature (Figs 2a, b and 3a). In Italy, the addition of biochar did not significantly affect the CO_2 flux in either trenched and untrenched subplots ($P > 0.05$; Table 2). In the UK site, R_{tot} was significantly higher with biochar, while no effect of biochar was detected for R_h (Table 2).

The isotopic signature of the CO_2 efflux emitted from biochar-treated plots was always significantly greater than that of CO_2 emitted from control plots (Fig. 5), with the only exception of August 23, 2012 and May 8, 2012 (for R_{tot} only) at the Italian site (Fig. 5c). Furthermore, no interaction was found between soil biochar application and root exclusion treatment on $\delta^{13}CO_2$ efflux (Table S1). These two conditions were an essential prerequisite to apply the mass balance approach according to the two-source mixing model, where one source
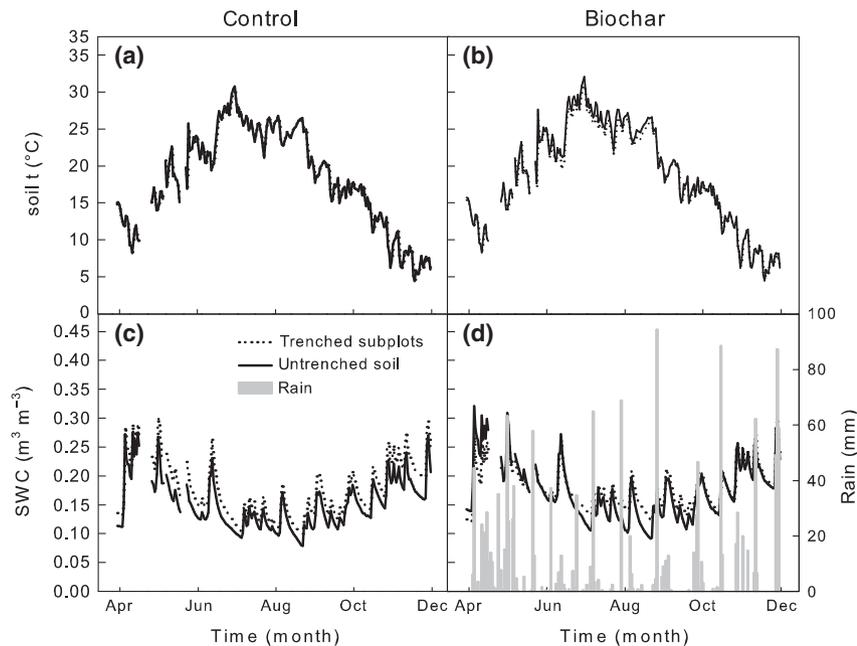

Fig. 2 Soil temperature (a, b) and water content (c, d) measured in the measured in biochar-treated (b, d) and untreated (a, c) plots and trenched subplots, in the Italian site. Total rainfalls in the area reported in plot d.
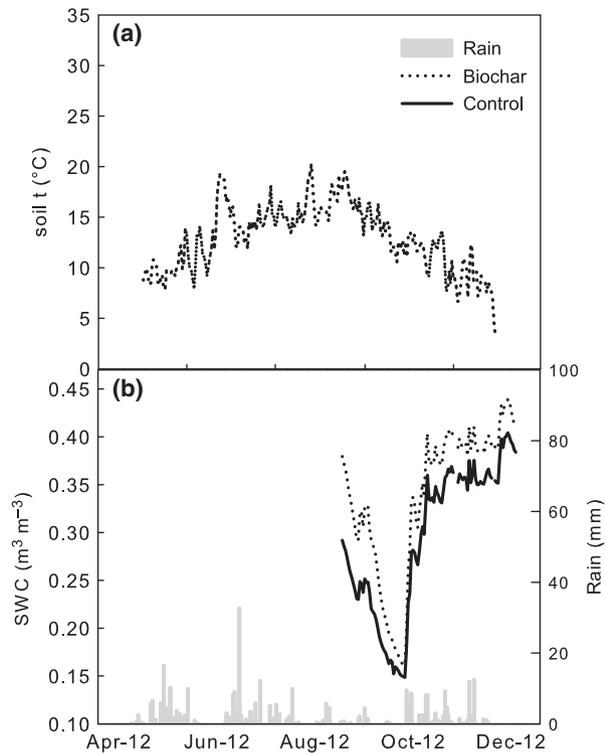
Fig. 3 Soil temperature (a) and water content (b) measured in biochar-treated and untreated plots, in the UK site. Soil temperatures registered in the trenched subplots and unternched soil were pooled together because no differences were detected between the two treatments. Total rainfalls in the area is reported in plot b.

was biochar and the other one was roots and SOM pooled together [Eqn (3)].

The percentage of soil respiration attributed to biochar (f_B) varied according to the site and sampling date (Fig. 6a, b). At the Italian site, it was between 7% and 36% with a clear seasonal trend especially in trenched plots (Fig. 6a). At the UK site, f_B varied between 12% and 32% with higher values in summer than in spring (Fig. 6b). At both sites, f_B was higher for R_{tot} than for R_h for most of the sampling dates (Fig. 6a, b). Thus, $R_{tot-biochar-derived}$ was higher than $R_{h-biochar-derived}$ (Table 2) and biochar decomposition curves were steeper in untrenched than trenched plots in both experimental sites (Fig. 7a,b). At the end of the experimental period, $R_{h-biochar-derived}$ accounted for the 7% and 3% of the carbon originally added by biochar application at the Italian and UK sites, respectively, while $R_{tot-biochar-derived}$ amounted to 9% and 8%, respectively (Fig. 7a, b).

Considering the different length of the experimental period at the two sites, in the trenched plots the daily degradation rate was higher at the Italian ($0.0288 \pm 0.0009\%$ day^{-1}) than at the UK site ($0.014 \pm 0.0003\%$ day^{-1}) (Table 2), while in the presence of plant

roots (control plots), the degradation rate was similar at both sites (0.039 ± 0.001 and $0.036 \pm 0.001\%$ day^{-1} at the UK and Italian site, respectively).

The $P_{eff-root}$ was +29 gC m^{-2} and +82 gC m^{-2} at Italian and UK site, respectively (Table 2). $R_{h-SOM-derived}$ amounted to 465 gC m^{-2} and 397 gC m^{-2} at the Italian and UK site, respectively, and at both sites it was lower than R_h. Therefore, the $P_{eff-biochar}$ was -54 gC m^{-2} (10% of R_h) at the Italian site and -66 gC m^{-2} (14% of R_h) at the UK site (Table 2).

Discussion

Generally, the application of trenching increases SWC, because of the absence of plant water uptake in the trenched plots (Kuzyakov & Larionova, 2005). This effect was observed in the Italian site, in particular in the summer period, only when biochar was applied (Fig. 2d). In the same period, soil T was decreased in the trenched subplots probably because of an enhanced evaporation from the trenched plots (Fig. 2b).

Considering that we found a positive relationship between soil respiration and SWC in both sites, a higher SWC in trenched and biochar-treated plots probably led to an overestimation of R_hB, and consequently to an underestimation of the $P_{eff-biochar}$ [Eqn (5)]. Nevertheless, the difference in SWC was so small and limited to a short-time period that the underestimation of negative priming effects was likely negligible. An increase in soil respiration after biochar addition has been previously observed in both lab (Kolb et al., 2009; Kuzyakov et al., 2009; Zimmerman, 2010; Cross & Sohi, 2011; Hale et al., 2011; Rogovska et al., 2011; Zavalloni et al., 2011) and field experiments (Jones et al., 2012; Ventura et al., 2013). This increase in soil CO_2 efflux has been related to the degradation of the labile fraction of biochar, such as bio-oils and condensation products (Thies & Rillig, 2009), or to the stimulation of SOM decomposition (Zimmerman, 2010; Luo et al., 2011). In the present study, at the Italian site, the cumulative CO_2 fluxes were not affected by soil biochar application (Table 2), since the CO_2 emission due to biochar decomposition was offset by a reduction in SOM decomposition. This result is in accordance with laboratory incubation studies under controlled conditions using the same biochar (Naisse et al., 2014). An increase in R_{tot} cumulative flux was observed at the UK site (Table 2).

With the exception of an initial phase characterized by a low decomposition rate at Italian site, the dynamics of biochar degradation can be well described by a negative double exponential function (Fig. 7). This agrees with the conceptual model for degradation of fresh biochar (Zimmerman, 2010),
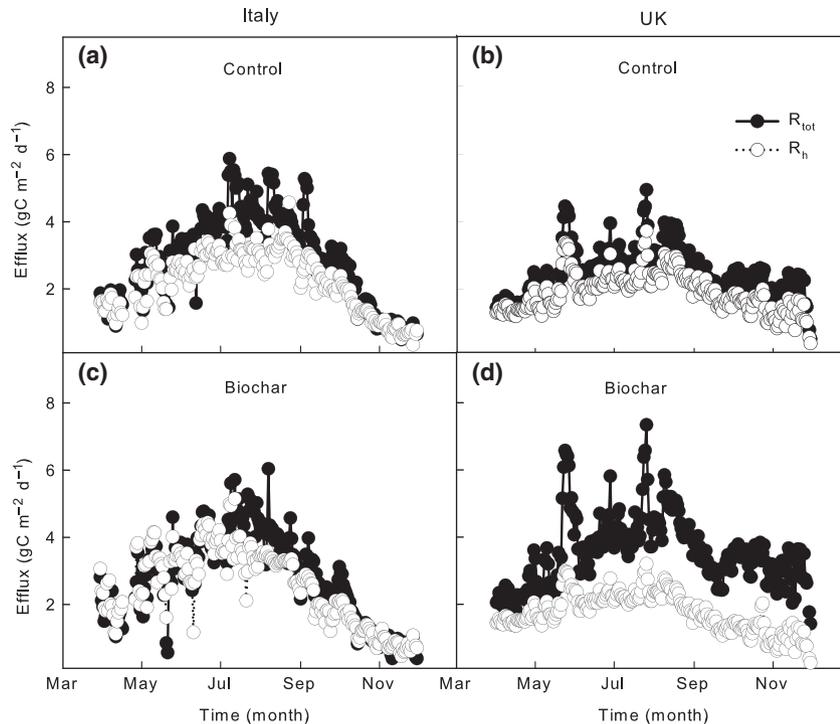
Fig. 4 Daily total (R_{tot}) and heterotrophic (R_h) soil respiration fluxes in control (a, b) and biochar (c, d) treatments for Italian and UK sites, respectively. Biochar was applied on March 30th and June 19th in Italy and UK, respectively.

whereby the biochar would consist of two pools: an aliphatic portion that is more readily mineralized and an aromatic one that is oxidized more slowly. The initial phase with low biochar decomposition rate was also observed by Bai *et al.* (2013) and Hamer *et al.* (2004) in two laboratory incubation experiments and related to the time needed by microorganisms to colonize biochar before degrading it.

Both sites showed higher decomposition rates than those previously reported by Kuzyakov *et al.* (2009). Naisse *et al.* (2014) in an incubation experiment, found a lower decomposition rate for the same biochar used in the present study. Several factors could have enhanced biochar decomposition rate under field conditions in comparison with controlled lab conditions; among them the inputs of fresh organic matter from plants (Keith *et al.*, 2011; Luo *et al.*, 2011) and the frequent abrupt variations of SWC have been suggested (Nguyen *et al.*, 2010). In the absence of plant roots, a higher biochar degradation rate was observed at the Italian site in comparison to the UK site (Fig. 7b). This could be explained by the different climatic conditions at the two sites, in particular to the higher soil temperature recorded in Italy (Figs 2 and 3). Mean annual temperature was suggested as one of the most important drivers of the natural

oxidation of charcoal in soil (Glaser & Amelung, 2003; Cheng *et al.*, 2008b).

The higher contribution of biochar-derived respiration to total CO_2 efflux (Fig. 6) and the higher decomposition rate in presence of roots (Fig. 7; Table 2) suggest a priming effect of roots on biochar decomposition. Many authors have found that root activity can stimulate SOM degradation (Kuzyakov, 2002; Schweinsberg-mickan *et al.*, 2012; Pausch *et al.*, 2013), although the underpinning mechanisms have not yet been completely clarified. It is likely that a combination of these mechanisms could have affected biochar decomposition as well. In fact, biochar decomposition has been shown to be higher after the addition of labile substrates such as glucose (Hamer *et al.*, 2004; Nocentini *et al.*, 2010) or fresh organic matter (Keith *et al.*, 2011; Luo *et al.*, 2011). This effect has been explained by the cometabolism concept, whereby the stimulation of microbial growth and enzyme production induced by the added substrates would increase the biochar decomposition (Hamer *et al.*, 2004). Plants can strongly influence the structure of soil microbial communities, and differentiate the rhizosphere microbial community from that of the surrounding soil (Bulgarelli *et al.*, 2013). Therefore, the root-induced priming effect on biochar decomposition could be due to a shift towards a more efficient biochar-

Table 2 Carbon fluxes and estimated daily decay rate (% day^{-1}) in the two experimental sites. All values are referred to the total number of the expected days (246). See material and methods section for more details on data analysis and gap-filling procedure

		Site	
	Unit	Italy	UK
R_{tot}	g C m^{-2}	668 ± 50	591 ± 70
$R_{tot}B$	g C m^{-2}	649 ± 100	856 ± 28
R_h	g C m^{-2}	519 ± 34	463 ± 87
R_hB	g C m^{-2}	585 ± 14	445 ± 55
$R_{tot\text{-}biochar\text{-}derived}$	g C m^{-2}	149 ± 6	130 ± 3
$R_{h\text{-}biochar\text{-}derived}$	g C m^{-2}	120 ± 4	48 ± 1
$P_{eff\text{-}root} = R_{tot\text{-}biochar\text{-}derived} - R_{h\text{-}biochar\text{-}derived}$	g C m^{-2}	29 ± 7	82 ± 3
$R_{h\text{-}SOM\text{-}derived} = R_hB - R_{h\text{-}biochar\text{-}derived}$	g C m^{-2}	465 ± 15	397 ± 55
$P_{eff\text{-}biochar} = R_{h\text{-}SOM\text{-}derived} - Rh$	g C m^{-2}	−54 ± 37	−66 ± 103
Biochar decay rate, untrenched soil	% day^{-1}	0.0362 ± 0.0009	0.0392 ± 0.0011
Biochar decay rate, trenched soil	% day^{-1}	0.0288 ± 0.0009	0.0144 ± 0.0003

Values are reported as mean ± standard error among the treatments ($n = 3$). Standard errors for biochar-derived C effluxes were calculated according to Phillips & Gregg (2001).
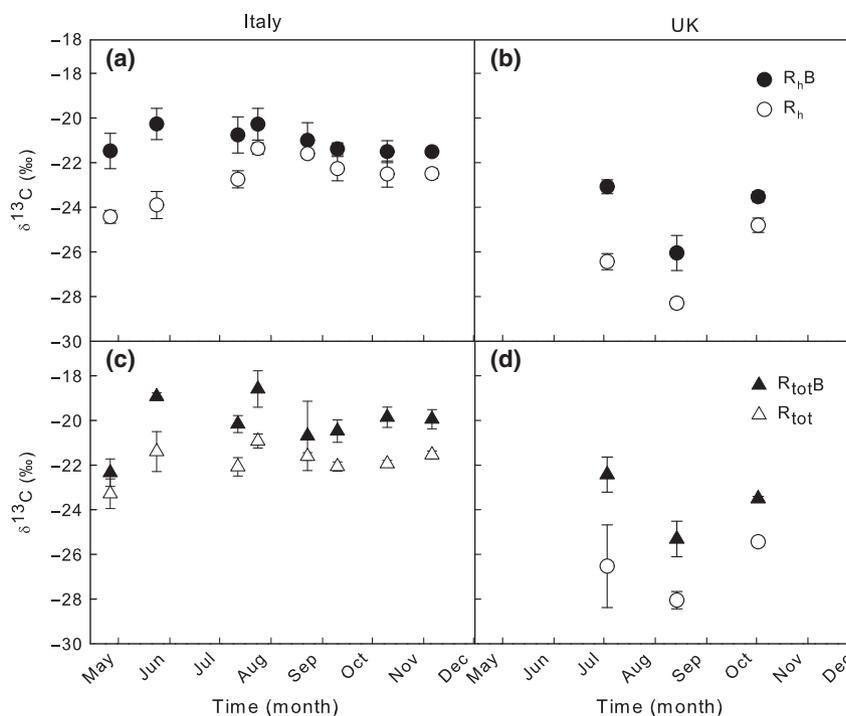

Fig. 5 Isotopic signature ($\delta^{13}C$) of total (c, d) and heterotrophic (a, b) CO_2 flux measured on biochar-treated plots ($R_{tot}B$ and R_hB, respectively) and on untreated control plots (R_{tot} and R_h, respectively), at the different sampling dates at the Italian (a, c) and UK (b, d) sites. Vertical bars represent standard error.

decomposing microbial community. The different plant species and rhizodeposits could explain why in United Kingdom the decomposition rate was higher than in Italy, notwithstanding the lower temperature recorded in the latter site.

The present study showed a small decrease in SOM decomposition after soil biochar addition (Table 2). This

negative priming effect was also observed during a laboratory incubation with the same biochar (Naisse et al., 2014). Also Liang et al. (2010) found a decrease in mineralization of added organic matter in a biochar-rich Amazonian Anthrosol. Similarly, Cross & Sohi (2011) found an inhibition of SOM decomposition during biochar incubation experiments with two different soils.
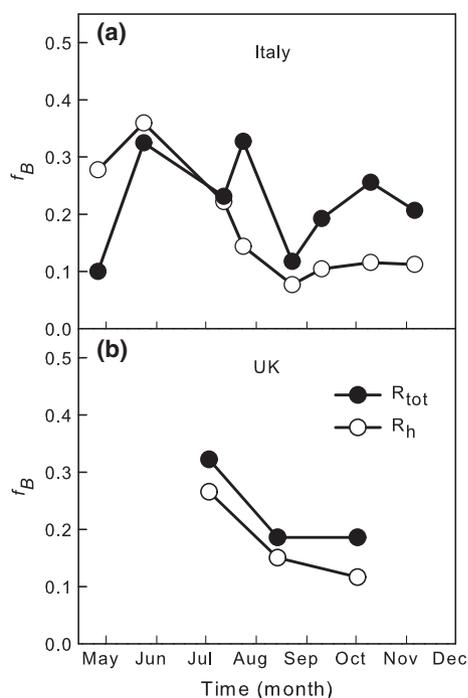
Fig. 6 Proportion (f_B) of biochar-derived CO_2 efflux on total (R_{tot}) and heterotrophic (R_h) flux, calculated at the different sampling dates at the Italian (a) and UK (b) sites.

Zimmerman *et al.* (2011), studying biochars produced from different feedstocks at different temperatures, observed a SOM protection effect of high-temperature biochars. It is well known that biochar surfaces and pores can absorb SOM molecules and protect them from decomposers (Zimmerman *et al.*, 2011). The adsorption affinity of biochar surfaces for SOM have been shown to increase with increased charring temperature and to be higher in grass biochar in comparison with wood biochar (Kasozi *et al.*, 2010). As we used a high-temperature biochar (1200 °C), we can suppose a high surface affinity of our biochar with SOM and consequently a high protective potential against biotic and abiotic oxidation. However, this protective effect of gasification char is likely to be short-lived and decrease after physical weathering during prolonged field exposure (Naisse *et al.*, 2014). Biochars produced at high temperatures have a high microporosity, which has been suggested to play a role in the inhibition of the SOM mineralization (Brewer *et al.*, 2011, 2014). Micropores may in fact be less accessible by microorganisms and protect absorbed organic matter against the microbial degradation (Ameloot *et al.*, 2013).

Without a robust evidence base of field data, evaluating the carbon mitigation potential of biochar technology, its diffusion and social acceptance is not justified.
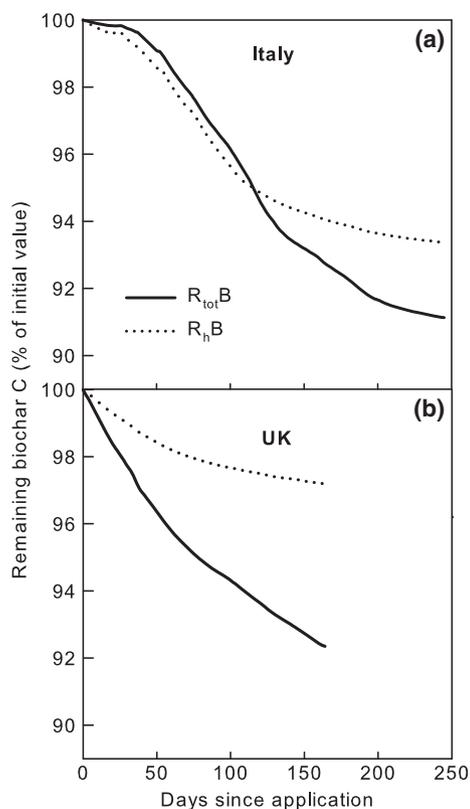

Fig. 7 Remaining amount of biochar-C (expressed as % of the initial amount added to soil), at the Italian (a) and UK (b) experimental sites, on undisturbed soil (soild line) and in trenched subplots, lacking roots (dotted line).

In this framework, multi-site field experiments aimed at assessing the biochar stability in field condition are crucial.

In the present article, regardless of the experimental site, biochar showed low decomposition rates and a protection effect on original SOM, confirming the carbon mitigation potential of this technology. However, the mechanisms that are behind the protective effect of biochar on SOM decomposition deserve to be investigated more deeply. Our field study showed that the presence of plant roots has a crucial effect on biochar stability through their priming effect. Therefore, laboratory incubations may overestimate the C sequestration potential of biochar. Similarly, as the positive priming effect of roots on biochar degradation could reduce or compromise the C-sink potential of biochar technology in a long-term perspective, the interaction between root activity and biochar stability has to be studied in depth and in long-term field experiments. The study of the change in microbial community induced by plant roots could be the key to understand the mechanisms underlying the observed priming effects.

Acknowledgement

References

Ameloot N, Graber ER, Verheijen FGA, De Neve S (2013) Interactions between biochar stability and soil organisms: review and research needs. *European Journal of Soil Science*, **64**, 379–390.

Bai M, Wilske B, Buegger F *et al.* (2013) Degradation kinetics of biochar from pyrolysis and hydrothermal carbonization in temperate soils. *Plant and Soil*, **372**, 375–387.

Bird MI, Moyo C, Veenendaal EM, Lloyd J, Frost P (1999) Stability of elemental carbon in a savanna soil. *Global Biogeochemical Cycles*, **13**, 923–932.

Brewer CE, Unger R, Schmidt-Rohr K, Brown RC (2011) Criteria to select biochars for field studies based on biochar chemical properties. *BioEnergy Research*, **4**, 312–323.

Brewer CE, Chuang VJ, Masiello CA *et al.* (2014) New approaches to measuring biochar density and porosity. *Biomass and Bioenergy*, **66**, 176–185.

Brown RA, Kercher AK, Nguyen TH, Nagle DC, Ball WP (2006) Production and characterization of synthetic wood chars for use as surrogates for natural sorbents. *Organic Geochemistry*, **37**, 321–333.

Bruun S, Jensen ES, Jensen LS (2008) Microbial mineralization and assimilation of black carbon: dependency on degree of thermal alteration. *Organic Geochemistry*, **39**, 839–845.

Bulgarelli D, Schlaeppi K, Spaepen S, Loren Ver, van Themaat E, Schulze-Lefert P (2013) Structure and functions of the bacterial microbiota of plants. *Annual review of plant biology*, **64**, 807–838.

Cheng C-H, Lehmann J, Thies JE, Burton SD (2008a) Stability of black carbon in soils across a climatic gradient. *Journal of Geophysical Research*, **113**, G02027.

Cheng C-H, Lehmann J, Engelhard MH (2008b) Natural oxidation of black carbon in soils: changes in molecular form and surface charge along a climosequence. *Geochimica et Cosmochimica Acta*, **72**, 1598–1610.

Cross A, Sohi SP (2011) The priming potential of biochar products in relation to labile carbon contents and soil organic matter status. *Soil Biology and Biochemistry*, **43**, 2127–2134.

Delle Vedove G, Alberti G, Zuliani M, Peressotti A (2010) Automated monitoring of soil respiration: an improved automatic chamber system. *Italian Journal of Agronomy*, **2**, 377–382.

Don A, Osborne B, Hastings A *et al.* (2012) Land-use change to bioenergy production in Europe: implications for the greenhouse gas balance and soil carbon. *GCB Bioenergy*, **4**, 372–391.

Glaser B, Amelung W (2003) Pyrogenic carbon in native grassland soils along a climosequence in North America. *Global Biogeochemical Cycles*, **17**, 1064.

Gurwick NP, Moore L, a, Kelly C, Elias P, (2013) A systematic review of biochar research, with a focus on its stability *in situ* and its promise as a climate mitigation strategy. *PLoS ONE*, **8**, e75932.

Hale S, Hanley K, Lehmann J, Zimmerman AR, Cornelissen G (2011) Effects of chemical, biological, and physical aging as well as soil addition on the sorption of pyrene to activated carbon and biochar. *Environmental Science & Technology*, **45**, 10445–10453.

Hamer U, Marschner B, Brodowski S, Amelung W (2004) Interactive priming of black carbon and glucose mineralisation. *Organic Geochemistry*, **35**, 823–830.

Hanson PJ, Edwards NT, Garten CT, Andrews JA (2000) Separating root and soil microbial contributions to soil respiration: a review of methods and observations. *Biogeochemistry*, **48**, 115–146.

Hilscher A, Knicker H (2011) Carbon and nitrogen degradation on molecular scale of grass-derived pyrogenic organic material during 28 months of incubation in soil. *Soil Biology and Biochemistry*, **43**, 261–270.

Hilscher A, Heister K, Siewert C, Knicker H (2009) Mineralisation and structural changes during the initial phase of microbial degradation of pyrogenic plant residues in soil. *Organic Geochemistry*, **40**, 332–342.

Jones DL, Rousk J, Edwards-Jones G, DeLuca TH, Murphy DV (2012) Biochar-mediated changes in soil quality and plant growth in a three year field trial. *Soil Biology and Biochemistry*, **45**, 113–124.

Joos O, Saurer M, Heim A, Hagedorn F, Schmidt MWI, Siegwolf RTW (2008) Can we use the CO2 concentrations determined by continuous-flow isotope ratio mass spectrometry from small samples for the Keeling plot approach? *Rapid Communications in Mass Spectrometry*, **22**, 4029–4034.

Kasozi GN, Zimmerman AR, Nkedi-Kizza P, Gao B (2010) Catechol and humic acid sorption onto a range of laboratory-produced black carbons (biochars). *Environmental science & technology*, **44**, 6189–6195.

Keith A, Singh B, Singh BP (2011) Interactive priming of biochar and labile organic matter mineralization in a Smectite-Rich Soil. *Environmental Science & Technology*, **45**, 9611–9618.

Kolb SE, Fermanich KJ, Dornbush ME, Dornbush KJ, Mathew E (2009) Effect of charcoal quantity on microbial biomass and activity in temperate soils. *Soil Science Society of America Journal*, **73**, 1173–1181.

Kuzyakov Y (2002) Review: factors affecting rhizosphere priming effects. *Journal of Plant Nutrition and Soil Science*, **165**, 382–396.

Kuzyakov Y, Larionova AA (2005) Root and rhizomicrobial respiration: A review of approaches to estimate respiration by autotrophic and heterotrophic organisms in soil. *Journal of Plant Nutrition and Soil Science*, **168**, 503–520.

Kuzyakov Y, Friedel JK, Stahr K (2000) Review of mechanisms and quantification of priming effects. *Soil Biology and Biochemistry*, **32**, 1485–1498.

Kuzyakov Y, Subbotina I, Chen H, Bogomolova I, Xu X (2009) Black carbon decomposition and incorporation into soil microbial biomass estimated by 14C labeling. *Soil Biology and Biochemistry*, **41**, 210–219.

Lehmann J (2007) Bio-energy in the black. *Frontiers in Ecology and the Environment*, **5**, 381–387.

Liang B, Lehmann J, Sohi SP *et al.* (2010) Black carbon affects the cycling of non-black carbon in soil. *Organic Geochemistry*, **41**, 206–213.

Luo Y, Durenkamp M, De Nobili M, Lin Q, Brookes PC (2011) Short term soil priming effects and the mineralisation of biochar following its incorporation to soils of different pH. *Soil Biology and Biochemistry*, **43**, 2304–2314.

Naisse C, Girardin C, Lefevre R, Pozzi A, Maas R, Stark A, Rumpel C (2014) Effect of physical weathering on the carbon sequestration potential of biochars and hydrochars in soil. *GCB Bioenergy.* doi: 10.1111/gcbb.12158

Ngao J, Epron D, Brechet C, Granier A (2005) Estimating the contribution of leaf litter decomposition to soil CO2 efflux in a beech forest using 13C-depleted litter. *Global Change Biology*, **11**, 1768–1776.

Nguyen BT, Lehmann J (2009) Black carbon decomposition under varying water regimes. *Organic Geochemistry*, **40**, 846–853.

Nguyen BT, Lehmann J, Hockaday WC, Joseph S, Masiello CA (2010) Temperature sensitivity of black carbon decomposition and Oxidation. *Environmental Science & Technology*, **44**, 3324–3331.

Nocentini C, Guenet B, Di Mattia E, Certini G, Bardoux G, Rumpel C, DiMattia E (2010) Charcoal mineralisation potential of microbial inocula from burned and unburned forest soil with and without substrate addition. *Soil Biology and Biochemistry*, **42**, 1472–1478.

Novak JM, Busscher WJ, Watts DW, Laird DA, Ahmedna MA, Niandou MAS (2010) Short-term CO2 mineralization after additions of biochar and switchgrass to a Typic Kandiudult. *Geoderma*, **154**, 281–288.

Pausch J, Zhu B, Kuzyakov Y, Cheng W (2013) Soil Biology & Biochemistry Plant inter-species effects on rhizosphere priming of soil organic matter decomposition. *Soil Biology and Biochemistry*, **57**, 91–99.

Phillips DL, Gregg JW (2001) Uncertainty in source partitioning using stable isotopes. *Oecologia*, **127**, 171–179.

Qi Y, Xu M (2001) Separating the effects of moisture and temperature on soil CO2 efflux in a coniferous forest in the Sierra Nevada mountains. *Plant and Soil*, **237**, 15–23.

Rogovska N, Laird D, Cruse R, Fleming P, Parkin T, Meek D (2011) Impact of biochar on manure carbon stabilization and greenhouse gas emissions. *Soil Science Society of America Journal*, **75**, 871–879.

Schweinsberg-mickan MS, Jörgensen RG, Müller T (2012) Rhizodeposition : its contribution to microbial growth and carbon and nitrogen turnover within the rhizosphere. *Journal of Plant Nutrition and Soil Science*, **175**, 750–760.

Singh BP, Cowie AL (2014) Long-term influence of biochar on native organic carbon mineralisation in a low-carbon clayey soil. *Scientific reports*, **4**, 3687.

Spokas KA (2010) Review of the stability of biochar in soils: predictability of O: C molar ratios. *Carbon Management*, **1**, 289–303.

Takahashi Y, Liang N (2007) based sampling technique for determination of carbon stable isotope ratio of soil respired CO2 and evaluation of influence of CO2 enrichment in chamber headspace. *Geochemical Journal*, **41**, 493–500.

Thies JE, Rillig MC (2009) Characteristics of biochar: biological properties. In: *Biochar for environmental management: science and technology* (eds Lehmann J, Joseph S), pp. 85–106. Earthscan, London, UK.

Ventura M, Zhang C, Baldi E, Fornasier F, Sorrenti G, Panzacchi P, Tonon G (2013) Effect of biochar addition on soil respiration partitioning and root dynamics in an apple orchard. *European Journal of Soil Science*, **65**, 186–195.

Viger M, Hancock RD, Miglietta F, Taylor G (2014) More plant growth but less plant defence? First global gene expression data for plants grown in soil amended with biochar. *Global Change Biology Bioenergy*, **6**, 1–15.

Wardle DA, Nilsson M-C, Zackrisson O (2008) Fire-derived charcoal causes loss of forest humus. *Science*, **320**, 629.

Zavalloni C, Alberti G, Biasiol S, Vedove GD, Fornasier F, Liu J, Peressotti A (2011) Microbial mineralization of biochar and wheat straw mixture in soil: a short-term study. *Applied Soil Ecology*, **50**, 45–51.

Zimmerman AR (2010) Abiotic and microbial oxidation of laboratory-produced black carbon (biochar). *Environmental science & technology*, **44**, 1295–1301.

Zimmerman AR, Gao B, Ahn M-Y (2011) Positive and negative carbon mineralization priming effects among a variety of biochar-amended soils. *Soil Biology and Biochemistry*, **43**, 1169–1179.

Zimmermann M, Bird MI, Wurster C *et al.* (2012) Rapid degradation of pyrogenic carbon. *Global Change Biology*, **18**, 3306–3316.

Supporting Information

Additional Supporting Information may be found in the online version of this article:

Figure S1. Relationship of the Keeling plot intercepts (δ^{13}C of the respired CO_2) obtained from the manual sampling and analysis by IRMS and direct measurement with CRDS. The dashed line represent 1 : 1 relationship.

Table S1. Analysis of variance (ANOVA) for the isotopic signature (δ^{13}C) of the CO_2 emitted from soil, for each sampling date.